Available online at www.sciencedirect.com

SciVerse ScienceDirect

Ceramics International 39 (2013) 3747–3751

CERAMICS INTERNATIONAL

www.elsevier.com/locate/ceramint

Effects of $Bi(Zn_{0.5}Zr_{0.5})O_3$ addition on the structure and electric properties of $BaTiO_3$ lead-free piezoelectric ceramics

Xiuli Chen*, Yiliang Wang, Fen He, Huanfu Zhou, Liang Fang*, Laijun Liu

State Key Laboratory Breeding Base of Nonferrous Metals and Specific Materials Processing, Key Laboratory of Nonferrous Materials and New Processing Technology, Ministry of Education, Guilin University of Technology, Guilin 541004, China

Received 13 September 2012; received in revised form 16 October 2012; accepted 16 October 2012
Available online 27 October 2012

Abstract

$(1-x)BaTiO_3$–$xBi(Zn_{0.5}Zr_{0.5})O_3$ [$(1-x)$BT–xBZZ, $0.01 \le x \le 0.09$] lead-free piezoelectric ceramics were prepared by solid-state reaction method. The effects of $Bi(Zn_{0.5}Zr_{0.5})O_3$ addition on the crystal structure and electric properties of the $BaTiO_3$ ceramics have been investigated. X-ray diffraction demonstrated that the samples exhibited a tetragonal to pseudocubic phase transition. The lattice parameters were found to increase with increasing the amount of BZZ content. Dielectric measurements revealed that the Curie temperature (T_c) shifted to higher temperature with increasing x. Furthermore, the ceramic with $x=0.01$ exhibited relatively good electrical properties with $d_{33}=195$ pC/N, $k_p=17.7\%$, $P_r=14.5$ lC/cm^2, and $E_c=11.13$ kV/cm.

Keywords: C. Dielectric property; C. Piezoelectric property; D. $BaTiO_3$; Temperature stability

1. Introduction

Recently, demands for thin dielectric layer less than 1 μm for high-capacitance and small-size multilayer ceramic capacitors (MLCC) continue to increase for automotive applications, such as the programmed fuel injection engine, electronic control unit, and anti-lock brake system [1–7]. For MLCC applications, dielectric materials must be electrically insulating ($>10^{10}$ Ωcm) and possess high dielectric constants (>1000) at room temperature [8]. As a ferroelectric perovskite compound, Barium titanate ($BaTiO_3$, BT) has been reported as a desirable material for MLCC applications due to its high dielectric constant at room temperature. However, there are three dielectric anomalies associated with phase transitions at −90 °C, 0 °C, and 125 °C for BT ceramic [9]. These anomalies cause large changes in dielectric constant near the transition temperature, particularly near Curie temperature, which restricted the applications of BT [10]. In addition, high sintering temperature (≥ 1300 °C) is another disadvantage for BT-based materials [11].

Consequently, many studies have been reported to modify the composition of BT-based materials to solve the above-mentioned problems. Mahajan et al. [12] reported that the substitution of Zr for Ti could increase the room temperature and peak dielectric constants of BT ceramics. Sun et al. [13] obtained a low temperature sintering BT-based ceramics by adding ZnO–B_2O_3 flux agent. Xiong et al. [14] and Zhang et al. [15] reported that the $Bi(Mg_{1/2}Ti_{1/2})O_3$ gave rise to an improved dielectric behavior of BT ceramics, indicating a great potential for high-temperature applications. The BT–$BiScO_3$–$Bi(Zn_{1/2}Ti_{1/2})O_3$ systems with a very stable dielectric constant greater than 1000 and low loss tangents (<0.01) over a wide range of temperature ($T<400$ °C) have been obtained by Huang et al. [16].

To summarize what has been mentioned above, it can be inferred that for BT ceramic, the substitution of A-site by Bi^{3+} and/or B-site by Mg^{2+}, Zn^{2+}, and Zr^{2+} can improve the dielectric property and reduce the sintering temperature. Hence, $Bi(Zn_{0.5}Zr_{0.5})O_3$ was chosen to improve the dielectric property of $BaTiO_3$ ceramic in this work. It is expected that a good temperature-stable dielectric material

*Corresponding author.
E-mail addresses: cxlnwpu@163.com (X. Chen), fanglianggl001@yahoo.cn (L. Fang).

0272-8842/$ - see front matter © 2012 Elsevier Ltd and Techna Group S.r.l. All rights reserved.
http://dx.doi.org/10.1016/j.ceramint.2012.10.211

with a low sintering temperature can be obtained. Moreover, the structures, densities, piezoelectric, and ferroelectric properties of BT–BZZ systems were also investigated.

2. Experimental

A conventional solid-state reaction method was used to prepare the $(1-x)BaTiO_3$–$xBi(Zn_{0.5}Zr_{0.5})O_3$ [$(1-x)$BT–xBZZ, $0.01 \le x \le 0.09$] ceramics. The raw materials were the analytical grade precursors ($BaCO_3$, TiO_2, ZrO_2, ZnO and Bi_2O_3). Stoichiometric proportions of the above precursors were mixed in alcohol medium using zirconia balls for 4 h. The mixtures were dried and calcined at 950 °C for 4 h. The resultant powders were mixed with 5 wt% of polyvinyl alcohol and pressed into pellets of 12 mm in diameter and 2 mm in height by uniaxial pressing under a pressure of 200 MPa. These pellets were surrounded by sacrificial powder of the same composition and were sintered for 4 h between 1200 and 1290 °C depending on composition.

The phase purity was determined by an X-ray diffractometer (XRD, Model X'Pert PRO, PANalytical, Almelo, the Netherlands) with Cu Kα radiation. Archimedes method was used to measure the bulk density. The microstructure of the obtained samples was investigated by scanning electron microscopy (SEM, Model JSM6380-LV, JEOL, Tokyo, Japan). Dielectric properties measurement was taken with an applied voltage of 500 mV over the frequency range of 40 Hz to 100 MHz from 350 K to 850 K with an impedance analyzer (Agilent 4294A). The piezoelectric coefficient d_{33} was recorded from 1-day aged samples using a quasi-static piezoelectric d_{33} meter (YE2730A, China). In order to get the temperature dependence of d_{33}, the 1-day aged samples were heated to different temperatures for 30 min, cooled down to room temperature and the d_{33} values were recorded. The polarization versus electric field hysteresis loops of selected composition was recorded at room temperature with a ferroelectric test system (TF Analyzer 2000). The resonant and anti-resonant frequencies for the planar and thickness vibration modes were measured using HP4294A impedance-phase gain analyzer, by which, the planar coupling coefficient (K_p) can be calculated using the following equation [17]:

$$K_p = \left[\frac{0.395 f_r}{(f_a - f_r) + 0.574}\right]^{-1/2}$$

where f_r and f_a are resonant and anti-resonant frequencies (Hz), respectively.

3. Results and discussion

Fig. 1 shows the XRD patterns of $(1-x)$BT–xBZZ ceramics ($0.01 \le x \le 0.09$) sintered at 1200–1290 °C for 4 h. All the peaks were indexed to a single perovskite structure without any secondary phases. The enlarged

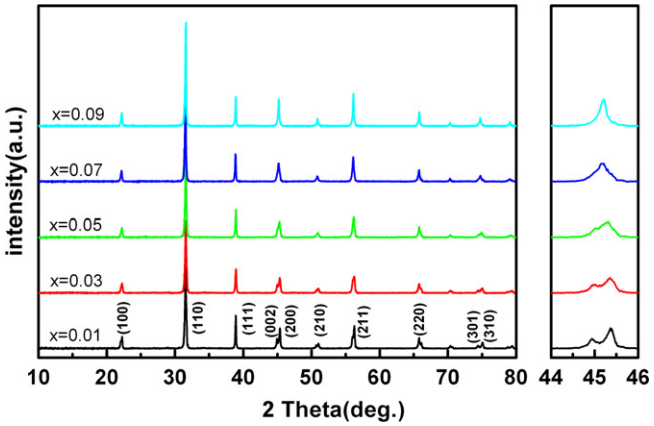

Fig. 1. X-ray diffraction patterns of $(1-x)$BT–xBZZ ceramics with $0.01 \le x \le 0.09$ sintered at 1200–1290 °C for 4 h.

XRD patterns of the powders in the range of 2θ from 44° to 46° clearly show that a pseudocubic phase appeared and increased gradually with increasing BZZ content. When $x \le 0.07$, a typical tetragonal phase can be formed and characterized by the separation of (200) and (002) peaks at around 45°, [18] which indicated that BZZ diffused into BT lattice to form a homogeneous solid solution (JCPDS: 005-0626). The pseudocubic phase can be obtained for the samples with $x=0.09$ with the merging of (200) and (002) peaks into a single (200) peak (JCPDS: 089-2475). Lattice parameters calculated based on XRD patterns of the samples are listed in Table 1. It can be seen that the unit cell volume increased with the increase of BZZ content. It is expected that Bi^{3+}(1.36 Å) should substitute for Ba^{2+} (1.61 Å) at A site, while the B-site ion Zn^{2+} (0.74 Å) and Zr^{2+} (0.8 Å) should substitute for Ti^{4+} (0.604 Å). The substitution on B-site may be the main effect on the BT lattice, leading to the expansion of the crystal unit cell.

Fig. 2 presents the surface morphology of $(1-x)$BT–xBZZ ceramics with (a) $x=0.01$, (b) $x=0.03$, (c) $x=0.05$, (d) $x=0.07$, (e) $x=0.09$. When $x=0.01$, the sample had a dense microstructure with small grains, as shown in Fig. 2(a). Dense microstructures with enlarged grains were developed with increasing x values. As a commonly used sintering additive, Bi_2O_3 can accelerate the sintering process, reduce the sintering temperature and enhance the escaping rate of pores [19]. From Table 1, it is clearly seen that the sintering temperature decreased with increasing BZZ content, indicating that the addition of BZZ can reduce the sintering temperature of the ceramics. Fig. 3 shows the variation of bulk density, theoretical density and relative density of the $(1-x)$BT–xBZZ ceramics. It can be seen that the bulk density remained almost unchanged with changing the BZZ content, but the theoretical density and relative density slightly increased with increasing BZZ content. It is well known that the atomic weight at A site is Ba < Bi, and at B site is Ti < Zn < Zr. According to the XRD analysis, the unit cell volumes increased with

Table 1
The lattice parameters, sintering temperatures and electrical properties of BT–BZZ ceramics.

Properties	$x=0.01$	$x=0.03$	$x=0.05$	$x=0.07$	$x=0.09$
Lattice parameter	$a=3.99656$ $c=4.02789$	$a=4.0035$ $c=4.02257$	$a=4.00759$ $c=4.02049$	$a=4.01109$ $c=4.01819$	$a=4.01353$
Sintering temperature (°C)	1290	1270	1250	1230	1200
d_{33} (pC/N)	195	160	142	92	33
K_p (%)	25.34	21.83	19.79	19.1	12.7

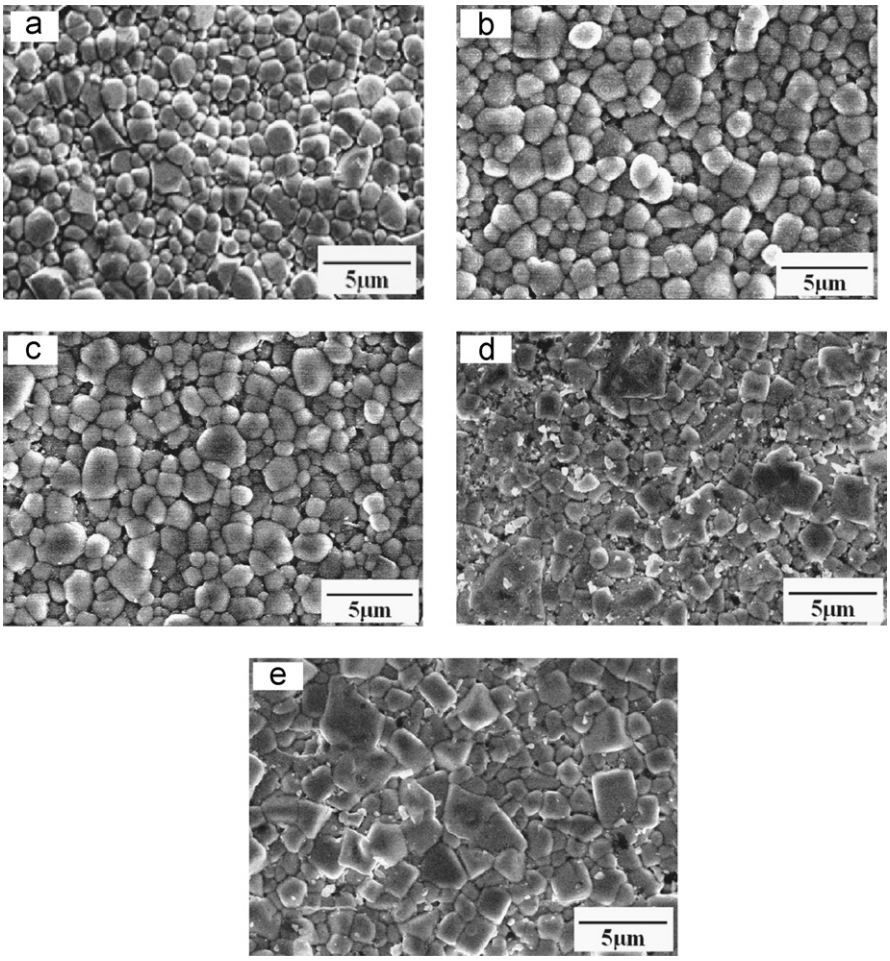

Fig. 2. The SEM images of $(1-x)$BT–xBZZ ceramics sintered at different temperature: (a) $x=0.01$, at 1290 °C; (b) $x=0.03$, at 1270 °C; (c) $x=0.05$, at 1250 °C; (d) $x=0.07$, at 1230 °C; (e) $x=0.09$, at 1200 °C.

increasing BZZ content. These comprehensive results lead to a slight change of theoretical density.

Fig. 4(a) shows dielectric constant as a function of temperature measured at 1 MHz. As BZZ was added to BT, two dielectric anomalies, corresponding to the ferroelectric–ferroelectric (T_{FE}) and ferroelectric–paraelectric phase transition (T_c), were observed and the maximum dielectric constant decreased significantly. Similar phenomenon was reported in the $BiScO_3$–$BaTiO_3$ and $BiScO_3$–$BaTiO_3$–$(K_{1/2}Bi_{1/2})TiO_3$ systems [20–22]. T_c increased with increasing BZZ content [as seen in the insert of Fig. 4(a)], which can be attributed to the enhanced structural distortion [23]. Furthermore, the dielectric temperature stability was improved. The dielectric constant characteristic of $(1-x)$BT–xBZZ ceramics as a function of BZZ content is shown in Fig. 4(b). It is clearly seen that the change of dielectric constant for $(1-x)$BT–xBZZ ceramics with $x=0.05$, 0.07 and 0.09 was around 15% over the temperature range from 25 to 125 °C. Especially for 0.95BT–0.05BZZ ceramic, the temperature variation of capacitance was within 15% in the temperature range of 23–150 °C, indicating a potential application in temperature-stable ceramic XnR (X and n are the minimum and maximum working temperature, respectively, R is maximum temperature coefficient of capacitance) capacitors.

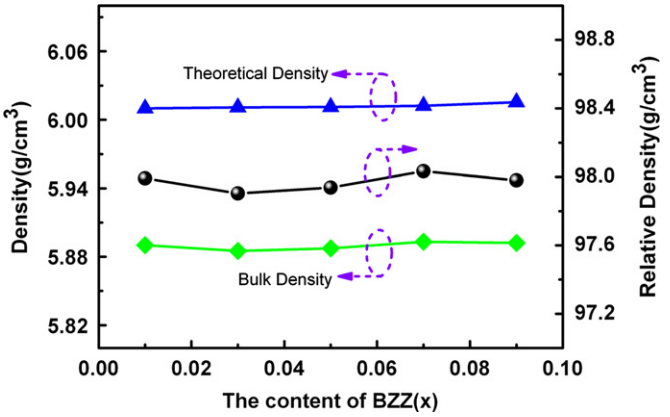

Fig. 3. Bulk density, theoretical density and relative density of $(1-x)$BT–xBZZ ceramics as a function of BZZ content.

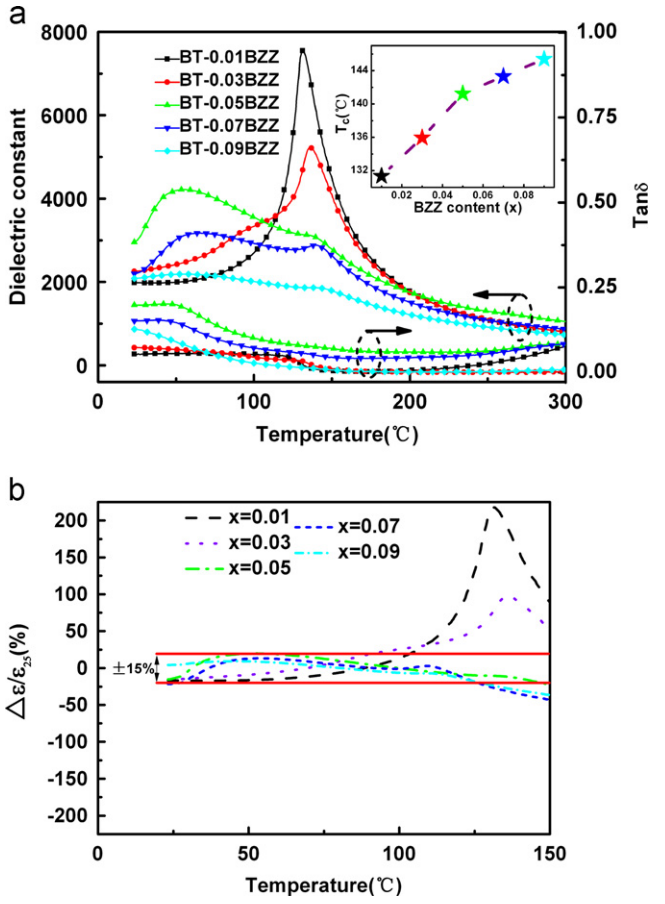

Fig. 4. (a) Temperature dependence of relative permittivity (ε′) for the $(1-x)$BT–xBZZ ($0.01 \le x \le 0.09$) ceramics measured at 1 MHz; (b) The dielectric constant-temperature characteristics of $BaTiO_3$-based ceramics as a function of BZZ content.

The variations of d_{33} and k_p of the $(1-x)$BT–xBZZ ceramics are also shown in Table 1. It can be observed that the d_{33} and k_p of the ceramics deteriorated seriously. According to the XRD analysis, Bi^{3+} should substitute for Ba^{2+} at A site, while at the B-site, Zn^{2+} and Zr^{2+} should substitute for Ti^{4+}. In addition, the crystal structure changed from tetragonal to pseudocubic, leading to a decrease in d_{33} and k_p. The thermal annealing behaviors of piezoelectric properties for $(1-x)$BT–xBZZ ($x=0.0$–0.09) ceramics are shown in Fig. 5. The thermal stability is very important for the practical applications. It can be seen that d_{33} showed a slight decrease when the annealing temperature was lower than T_c. But when the annealing temperature was close to T_c, d_{33} decreased rapidly. Moreover, it was also observed that T_c has been shifted to higher temperature, which agreed well with the result of dielectric properties, as seen in Fig. 4(a).

P–E hysteresis loops of the $(1-x)$BT–xBZZ ceramics at room temperature are shown in Fig. 6(a). All the samples exhibited saturated ferroelectric polarization hysteresis loops. Remnant polarization (P_r) and spontaneous polarization (P_s) decreased significantly with increasing BZZ content, as shown in Fig. 6(b), which may result from the deviation of Ti^{4+}, Zr^{2+} and Zn^{2+} from the center of the oxygen octahedrons. Furthermore, the results also confirm that the crystal structure of the samples with $x=0.09$ was not truly cubic but a pseudocubic structure, because perovskite material with cubic symmetry has no spontaneous polarization.

4. Conclusion

$(1-x)$BT–xBZZ ($0.01 \le x \le 0.09$) lead-free ceramics were synthesized via the solid-state processing technique. A systematic structural change from tetragonal phase to pseudocubic phase was observed near $x=0.05$. The phase transition temperatures (T_{FE} and T_c) shifted to higher temperatures with increasing x values. The results indicate that the ferroelectric phase of the $(1-x)$BT–xBZZ ceramics becomes more stable with increasing x values. When $0.03 \le x \le 0.09$, the samples possessed a temperature-stable relative permittivity and the value of $\Delta\varepsilon/\varepsilon_{25}$ was around 15% in the temperature range of 25–150 °C, indicating a potential application in XnR capacitors.

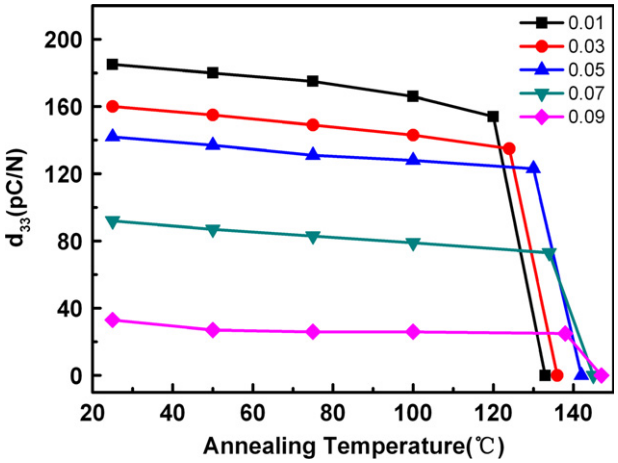

Fig. 5. Thermal annealing behaviors and aging characteristics of d_{33} of $(1-x)$BT–xBZZ ceramics with $0.01 \le x \le 0.09$.

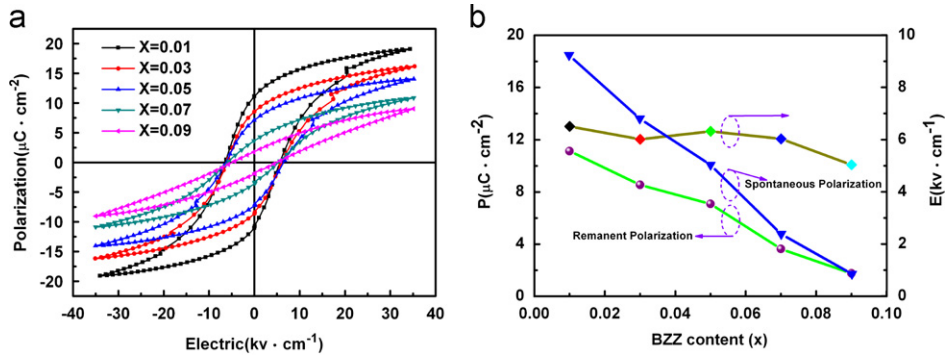

Fig. 6. Hysteresis loops of $(1-x)$BT–xBZZ ceramics with $0.01 \leq x \leq 0.09$. Insert shows the curves of coercive field E_c and remnant polarization P_r versus BZZ content.

Acknowledgment

This work was supported by the Natural Science Foundation of Guangxi (Nos. 2011GXNSFB018009, 2011GXNSFB018012 and 2012GXNSFDA053024), the Natural Science Foundation of China (Nos. 51102058, 50962004, 21061004, and 21261007), Research start-up funds Doctor of Guilin University of Technology (No. 002401003282).

References

[1] W.H. Lee, C.Y. Su, Journal of the American Ceramic Society 90 (2007) 3345–3348.
[2] H. Kishi, Y. Mizuno, T. Hagiwara, H. Orimo, H. Ohsato, Journal of Electroceramics 21 (2008) 22–28.
[3] S.S. Park, J.M. Kim, W.J. Chung, O.C. Shin, Journal of Central South University of Technology 18 (2011) 726–730.
[4] C.E. Lee, S.H. Kang, D.S. Sinn, H.I. Yoo, Journal of Electroceramics 13 (2004) 785–791.
[5] A.V. Polotai, T.H. Jeong, G.Y. Yang, E.C. Dickey, C.A. Randall, P. Pinceloup, A.S. Gurav, Journal of Electroceramics 23 (2009) 6–12.
[6] A.V. Polotai, T.H. Jeong, G.Y. Yang, E.C. Dickey, C.A. Randall, P. Pinceloup, A.S. Gurav, Journal of Electroceramics 18 (2007) 261–268.
[7] B. Tang, S.R. Zhang, X.H. Zhou, Y. Yuan, Journal of Materials Science: Materials in Electronics 18 (2007) 541–545.
[8] F.D. Morrison, D.C. Sinclair, A.R. West, International Journal of Inorganic Materials 3 (2001) 1205–1210.
[9] J. Chen, W. Jin, Y. Yao, Ferroelectrics 142 (1993) 153–159.
[10] D. Berlincourt, in: O.E. Mattiat (Ed.), Ultrasonic Transducer Materials: Piezoelectric Crystals and Ceramics, Plenum, London, 1971, pp. 100–124 (Chapter 2).
[11] H.I. Hsiang, C.S. Hsi, C.C. Huang, S.L. Fu, Materials Chemistry and Physics 113 (2009) 658–663.
[12] Sandeep Mahajan, O.P. Thakur, Chandra Prakash, K. Sreenivas, Bulletin of Materials Science 7 (2011) 1483–1489.
[13] C.K. Sun, X.H. Wang, C. Ma, L.T. Li, Journal of the American Ceramic Society 92 (2009) 1613–1616.
[14] B. Xiong, H. Hao, S.J. Zhang, H.X. Liu, M.H. Cao, Journal of the American Ceramic Society 94 (2011) 3412–3417.
[15] Q. Zhang, Z.R. Li, F. Li, Z. Xu, Journal of the American Ceramic Society 94 (2011) 4335–4339.
[16] C.C. Huang, D.P. Cann, X. Tan, N. Vittayakorn, Journal of Applied Physics 102 (2007) 044103–044105.
[17] M. Matsubara, T. Yamaguchi, W. Sakamoto, K. Kikuta, T. Yogo, S. Hirano, Journal of the American Ceramic Society 88 (2005) 1190–1196.
[18] K. Suzuki, K. Kijima, Journal of Materials Science 40 (2005) 1289–1292.
[19] Y. Shi, Z.G. Jin, Z.J. Cheng, X.Z. Wei, T.X. Xu, Journal of Chinese Ceramic Society 31 (2003) 571–574.
[20] H. Ogihara, C.A. Randall, S. Trolier-McKinstry, Journal of the American Ceramic Society 92 (2009) 1719–1724.
[21] H. Ogihara, C.A. Randall, S. Trolier-McKinstry, Journal of the American Ceramic Society 92 (2009) 110–118.
[22] J.B. Lim, S.J. Zhang, Namchul Kim, Thomas R. Shrout, Journal of the American Ceramic Society 92 (2009) 679–682.
[23] D. Fu, M. Endo, H. Taniguchi, T. Taniyama, M. Itoh, S. Koshihara, Journal of Physics: Condensed Matter 23 (2011) 075901.